EasyChair Preprint

№ 2044

Power Control Strategies of Grid Side Inverters Over Unbalanced Grid Faults in PMSG-Based Wind Turbines

P Parvathee Devi, D Narmitha and G Lakshmi Lavanya

November 28, 2019

Power Control Strategies of Grid Side Inverters Over Unbalanced Grid Faults in PMSG-Based Wind Turbines

P. PARVATHEE DEVI
Assistant Professor,
Dept of EEE,
SPMVV, Tirupati, AP.
Email:parvathi226@gmail.com

D.NARMITHA
Assistant Professor,
Dept of EEE,
SPMVV, Tirupati, AP.
dama.narmitha@gmail.com

G.LAKSHMI LAVANYA
PG Student,
Dept of EEE(PEDR),
SPMVV, Tirupati, AP.
lavanyagopavarapu@gmail.com

***Abstract*— The high level of penetration forces the wind turbines stay connected to the grid during the disturbances in order to enhance system stability. Requirements of grid codes for wind power integration will also be discussed regarding active power control, reactive power control and fault ride through (FRT) capability. For the MPPT, a proportional control loop is added to the torque control to reduce the influence of the inertia moment in the wind turbines, which can improve its dynamic performance. Furthermore, the grid side active power oscillation and dc-link voltage ripple can be suppressed by using the proposed controller. In this system, the entire control system by using proportional resonant controller to reduce the computational time. Simulation results showed the validity and efficiently of the proposed control approach in different conditions.**

***Index Terms*— Low-voltage ride-through(LVRT), grid faults, voltage sag, active power control, peak current limitation, maximum power point tracking (MPPT).**

I. INTRODUCTION

In the recent years, the wind power generation has been concerned as one of the most rapidly growing energy sources in the world since the natural resources are becoming exhausted. In the variable-speed wind turbine (WT) systems, a direct-drive wind energy conversion system based on PMSGs has a lot of advantages such as no gearbox, high precision, high power density, and simple control method, except initial installation costs. As the scale of wind farms becomes larger and larger, the condition of the grid-connected wind turbines is more important. Recently, some countries have issued the dedicated grid codes for connecting the wind turbine system to the grid. Also, the smart-grid and the micro-grid have been researched for the efficiency of the power management. However, the grid voltage in these systems is more fluctuated than that of the conventional grid. Therefore, an advanced control of the wind power generation system is required for the grid abnormal conditions. Several solutions have been proposed for the grid faults in the variable-speed wind turbine systems. For the low voltage ride-through (LVRT) purpose, a crowbar system consisting an external resistor is connected in the rotor-side of the doubly-fed induction generator (DFIG) to absorb the active power during the grid fault. The wind turbine keeps operating to produce the active power, whereas the reactive power or the voltage at the grid connection is controlled by the GSC. Nevertheless, during a grid fault and in the case of a weak grid, the GSC cannot provide sufficient reactive power or voltage support due to its small power capacity and there is a risk of voltage instability. Also, to guarantee the uninterrupted operation of a DFIG wind turbine during the grid faults, a static synchronous compensator (STATCOM) which is installed at the point of common coupling (PCC) has been used to inject the reactive power to the grid. However, it is not used alone for the DFIG ride-through capability since it cannot protect the rotor-side converter (RSC) during a grid fault. On the other words, it should be used in addition to the crowbar circuit which protects the RSC from the rotor over-current when the grid fault happens. This paper proposes a new control strategy for direct-driven MW-class high inertia PMSG based wind turbine operating in different conditions. In this structure, MPPT is implemented by GSC, and MSC controls dc-link voltage. By using this structure, the active crowbar in dc-link is eliminated. Also, the dual

current controller is designed for positive- and negative sequence components for GSC in order to deal with the asymmetrical faults. As a new contribution to earlier studies, this paper proposes a new upper limiter to keep the peak of currents of all phases in the safety limit. In addition, it permits the injection of the reactive current to the grid according to the reactive current requirement of grid codes in symmetrical and asymmetrical grid faults. In fact, by limiting the active power (active current), both negative sequence current and reactive current (according to grid code) can be injected to the grid. The limiters of active and reactive power references of GSC are calculated in the grid voltage sag conditions. Hence, The PMSG keeps out from MPPT in voltage sags, and GSC can be operated as STATCOM. In this situation, mechanical part of turbine-generator acts as an energy storage system. Therefore, the speed of wind turbine is increased (which is controlled by pitch angle in critical speed). It is noteworthy here that this control strategy is compatible with different grid codes. Moreover, the proposed structure has good performances in different types of asymmetrical faults. Furthermore, the grid side active power oscillation and dc-link voltage ripple can be suppressed by using proposed controller.

II.SYSTEM MODELING

A back-to-back converter consists of two voltage source converters(VSC) and a capacitor as shown in Fig.1. When operating in generator mode, the generator side converter operates as a rectifier and the grid side converter as an inverter. But as both converters are identical, power flow can be bi-directional.

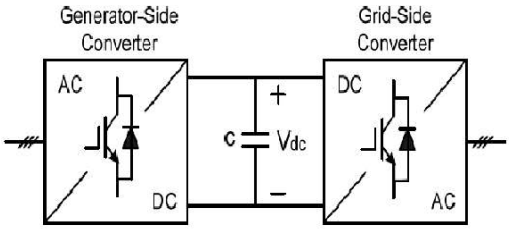

Fig. 1: Back To Back converter

But as the grid side is only considered in simulations, the model of the whole back-to-back converter is not needed. Consequently, the model of the grid side VSC is sufficient to carry out the simulations and is the only part considered in this section. The model of the VSC is an average model as the system includes a mechanical system making the time-frame of interest much longer than the switching time of the converter. Therefore, there is no need to have a switching model where the effect of switching adds little significance to the result. Its logical scheme was implemented as two sub-blocks, one for calculating the voltages and one for the currents. The two switches on the same branch will be commanded by a boolean signal (da, db, dc): a 1 value on the input will turn on the upper switch and turn off the lower, a 0 value will turn on the lower and turn off the upper one. In every instant three switches, one per leg will be on. The power converters, which are identical on both the generator- and grid-side, and linked through a dc-link, are classified as back-to-back (BTB) connected converters. Different BTB converters which can be used in the commercial WECS are summarized in Fig. 2. They perform a conversion of variable voltage/frequency output of the generator to dc, and then dc to ac, with fixed voltage/frequency for the grid connection. The power flow is bidirectional, and thus the BTB converters can be used with SCIG, PMSG and WRSG. The BTB converters are classified as low voltage (< 1 kV) and medium voltage (1− 35 kV) converters according to IEC 60038 standard. The most standard voltages used by many commercial wind turbine manufacturers for the LV grid connection are 690 V and 575 V.

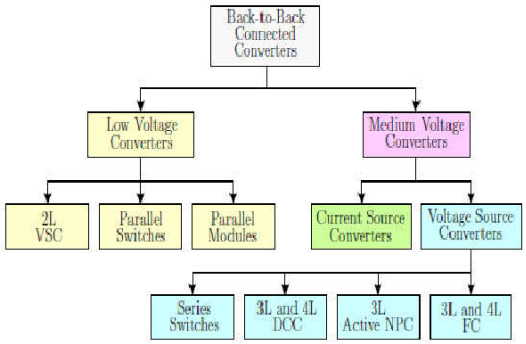

Fig. 2: Classification of back-to-back connected converters.

The considered wind energy conversion consists of four mai n parts: a wind turbine which extracts wind energy, PMSG which converts mechanical power into electrical power, BTB converter which transforms variable frequency signal to grid frequency by desired options, and finally a grid model (see Fig. 3).

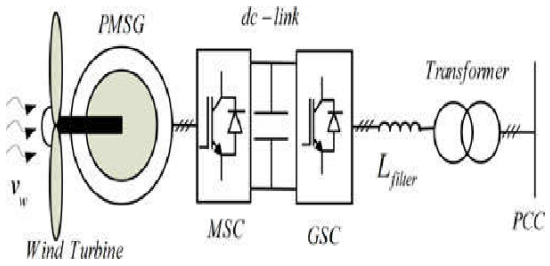

Fig. 3: Simplified scheme of co nsidered windenergy conversion system.

As shown in Fig. 3, the GSC is connected to the point of common coupling (PCC) by grid filter and couplin g transformer. This project proposes a new c ontrol strategy for direct-driven MW-class high inertia PMSG based wind turbine operating in different conditions. In this structur e, MPPT is implemented by GSC, and MSC controls dc-link voltage. By using this struc ture, the active crowbar in dc-link is eliminated. Also, the dual current controller is designed for positive- and negative-sequence components for GSC in order to deal with the asymmetr ical faults. As a new contribution to earlier studies, this project proposes a new upper limiter to keep the peak of currents of all phase s in the safety limit. In addition, it permits the injection of the reactive current to the grid ac cording to the reactive current requirement of grid codes in symmetrical and asymmetrical grid faults.

III. SIMULATION RESULTS

To comparison the mentioned numerical examples with real conditions, and also to show the good performances of proposed method, several sim ulations were performed in Matlab/Simulink s oftware.

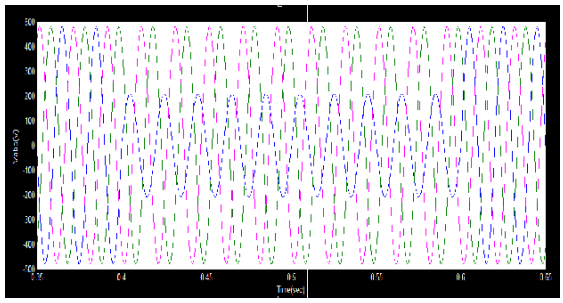

Fig. 4(a):

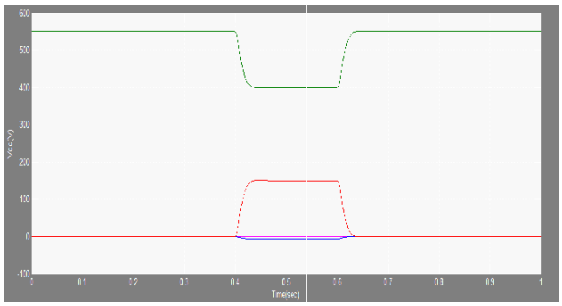

Fig. 4(b):

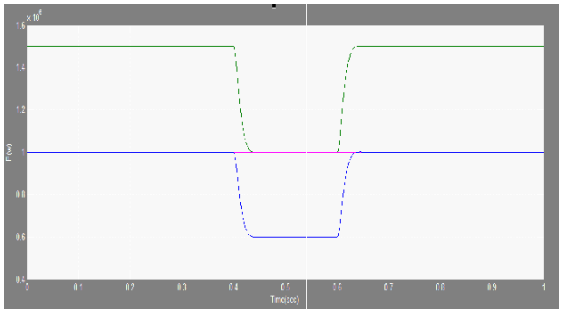

Fig. 4(c):

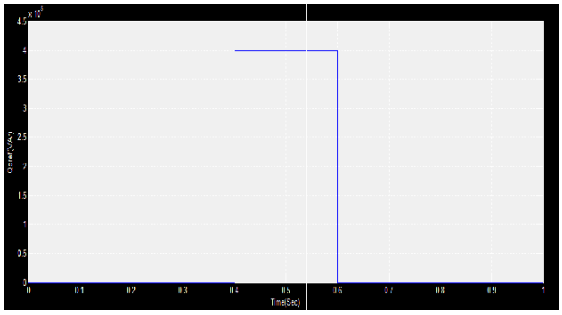

Fig. 4(d):

Fig. 4(a) PCC voltage, **(b)** PCC voltage in thesynchronous d-q coordinates, **(c)** Active power limitation (*Plim*), active power reference (*P0ref*), applied active power reference (*Pgridref*), and**(d)**Reactive power reference in onephase voltage sag.

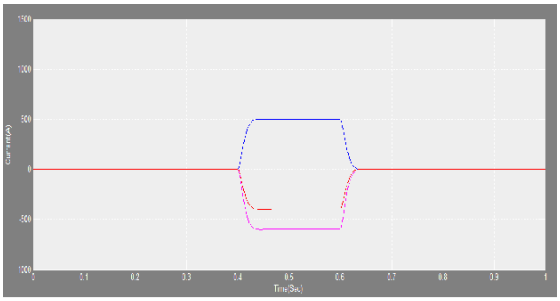

Fig. 5(a):

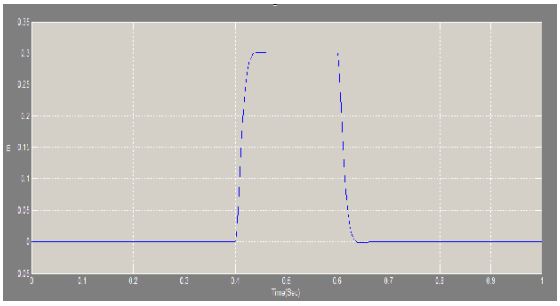

Fig. 5(b):

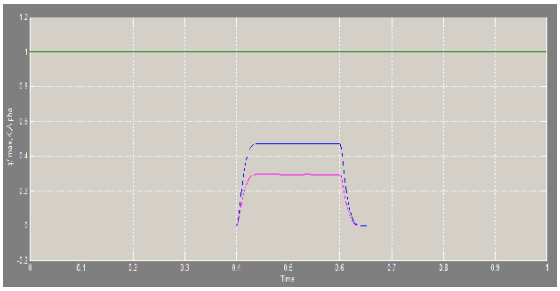

Fig. 5(c):

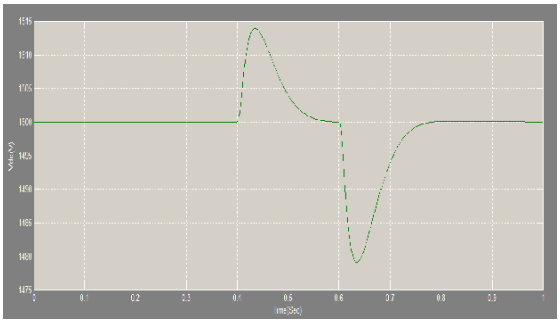

Fig. 5(d):

Fig. 5(a) The d-q components of positive-andnegative-sequences of GSC cu rrent, **(b)** The voltage unbalance factor (*m*), **(c)** Reactive power reference factor (κ), the reactive current to rated GSC current ratio (*Iq /Imax*) and(α), and **(d)** DC-link voltage in on e-phase voltage sag.

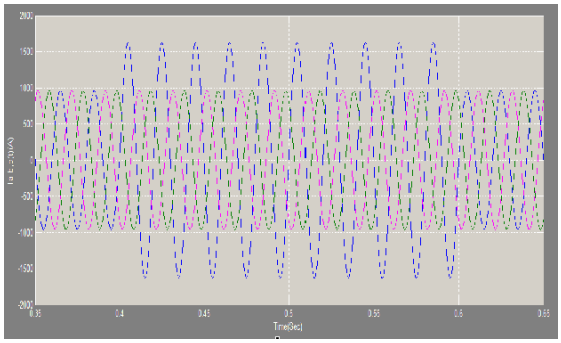

Fig. 6(a):

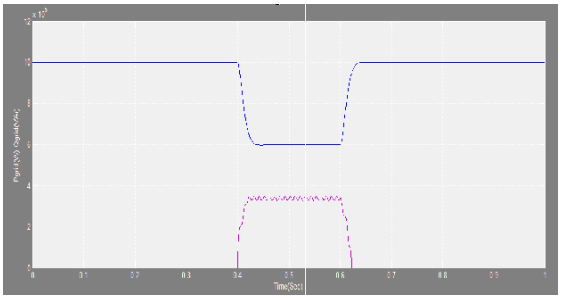

Fig. 6(b):

Fig. 6(a) Grid side current, **(b)** Grid activepower and grid reactive power in one-phase voltage sag.

A one-phase to ground fault was applied to the PCC in 10 s. As shown in Fig. 4(a), the one-phase volt age sag occurred in PCC. The PCC voltage w as transferred to d-q components, and then their positive- and negative-sequences were separated as shown in Fig. 4(b). Fig. 4(c) sho ws the active power limitation (*Plim*), active power reference (*P0ref*), and applied act ive power reference (*Pgridref*) as MPPT controller input. In fact, the active power referen ce will be limited in safety bound when volta ge sag occurs in the grid, and allowable active power reference (*Pgridref*) is used as active power reference. Also, according, the reactive power reference was calculated to implem ent reactive current injection according to grid code (see Fig. 4(d)). Fig. 5(a) illustrates the d-q components of positive- and negativ e-sequences of GSC current by applying the active power limiter. Fig. 5(b) shows the volt age unbalance factor equivalent to 0.3205 during voltage sag. As shown in Fig. 5(c), reactive current injection satisfies the requirement of reactive current in Danish grid code. Accord ing to Fig. 5(c), the ratio of *Iq+* to *I*max is more than the value of

reactive current to rated GSC cu rrent ratio (α), because α is calculated from the value of positive sequence of grid voltage and there are not negative sequences of current. However, the ratio of *Iq*+ to *I*max has negative sequence component of q-axis current. Finally, dc-link voltage is shown in Fig. 5(d). Because of the implementation of new control strategy, the dc-link voltage is limited in safety range without any external devices. Since dc-link voltage is controlled by MSC and a dual-current controller is used, the amplitude of second-order harmonic fluctuations decreases. Fig. 6(a) shows the grid side current of the GSC. As shown, the peak of each phase current is kept within the safe ty limit. This subject is one of the main contributions of this work. As mentioned before, to eliminate second-order component fluctuations of grid active power, *Pc*2 and *Ps*2 were set to zero; therefore, the second-order component fluctuations of grid active power is removed (see Fig. 6(b)). But, the fluctuations of reactive power of grid are retained. Henc e, the reactive power oscillates with 100 Hz as shown in Fig. 6(b). It is important to note that the average of reactive power in Fig. 6(b) is the same with the reactive power reference (*Q* 0*ref*) in Fig. 4(d). Accordingly, reactive curr ent injection is performed in agreement with th e Danish grid code.

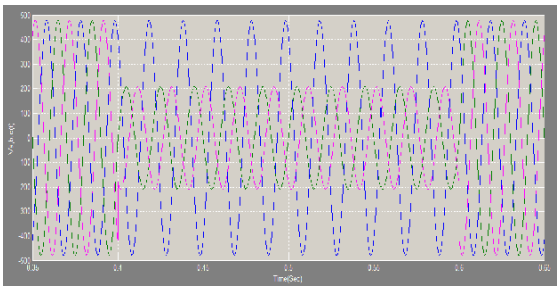

Fig. 7(a):

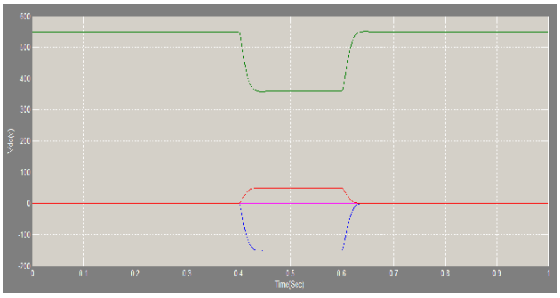

Fig. 7(b):

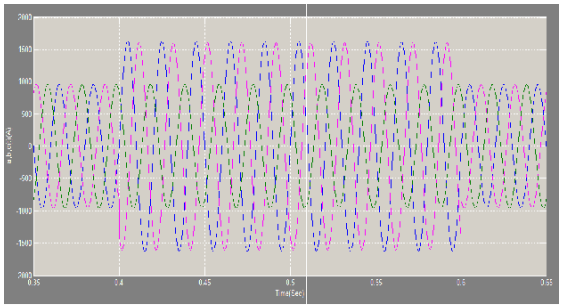

Fig. 7(c):

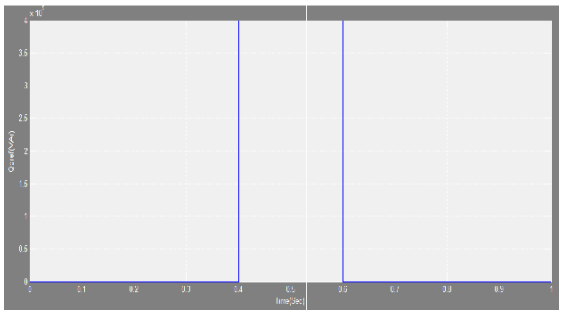

Fig. 7(d):

Fig. 7(a) PCC voltage, **(b)** PCC voltage in thesynchronous d-q coordinates, **(c)** Active power limitation (*Plim*), active power reference (*P0ref*), applied active power reference (*Pgridref*), and**(d)**Reactive po wer reference in twophase voltage sag.

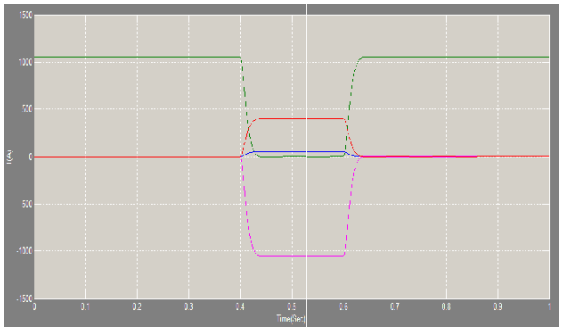

Fig. 8(a):

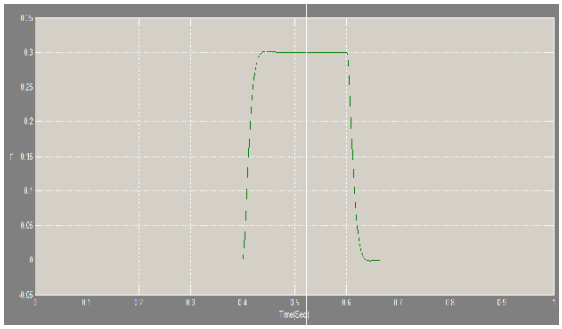

Fig. 8(b):

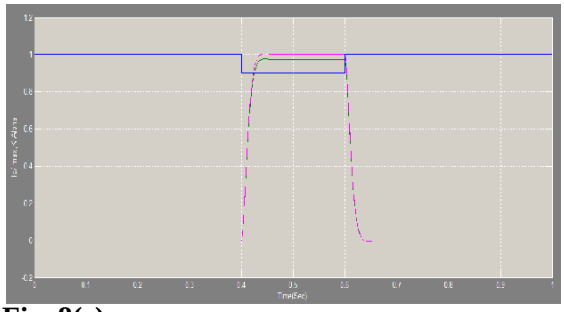

Fig. 8(c):

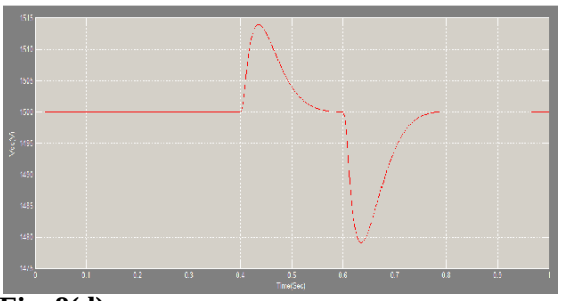

Fig. 8(d):

Fig:8.(a) The d-q components of positive-andnegative-sequences of GSC current, **(b)** The voltage unbalance factor (*m*), **(c)** Reactive power reference factor (*κ*) the r eactive current to rated GSC current ratio (*Iq* +- */Imax*) and(*α*), and **(d)** DC-link voltage in two-phase voltage sag.

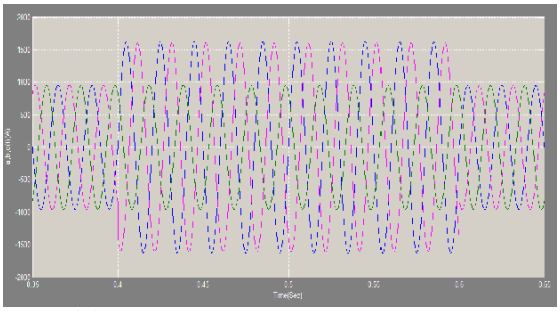

Fig. 9(a):

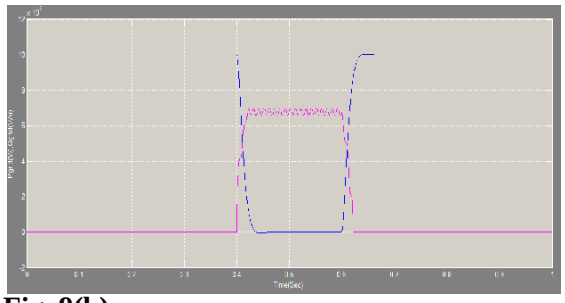

Fig. 9(b):

Fig:9.(a) Grid side current, (b) Grid active power and grid reactive power in two-phase voltage sag.

According to this scenario, unbalanced two phase vo ltage occurred in 10 s (see Fig. 7(a)). Fig. 7(b) shows PCC voltage in the synchronous d-q reference frame. As earlier menti oned, the important issue is limiting the gen erated PMSG active power in grid side vooltage sag. In this condition, the reference power does not track MPPT; see Fig. 7(c). In fact, the voltage drops close to 50%; Hence, the active current must be reduced to zero and the GSC should inject reactive current equal to rated current of GS C. To generate the required reactive current, the reactive power reference is obtained, acc ording to Fig. 7(d).

Owing to the pos itive sequence of d-axis current, *Id* +, is as sociated with active power, it attains a level of zero in this scenario. Also, the positive sequence of q-axis current, *Iq* + shou ld reach maximum allowable value.

Due to the pr esence of negative sequence in unbalanc ed voltage sags, negative sequence of current must be injected to remove second-order active power fluctuations, see Fig. 8(a). Fig. 8(b) shows voltage unbalan ce factor which is more than 40%. The reac tive current to rated GSC current ratio (*α* an d *Iqf /I*max) and the reactive power reference factor, *κ*, are shown in Fig. 8(c). Due to th e deep voltage sag, according to grid code, *α* and *Iqf /I*max should approach a value of 1. But in this situation, *Q*0 *ref* exce eded the allowable value. Hence, the reactive power reference factor is reduced to pre vent over-current in GSC. However, the deep voltage sag occurred in the grid side ; but dc-link voltage remained in the safety region without any external devices accordin g to Fig. 8(d).

By using the d esigned limiter, the peak of three phase curr ents is kept in safety bound; see Fig. 9(a). On the other hand, the second-order fluctuations of grid active power will be removed as shown in Fig. 9(b). The*Qgrid* is simil ar to*Q*0 *ref* ; but it contains second-order flu ctuations due to the presence of negative seq uence of current and voltage (see Fig. 9(b)).

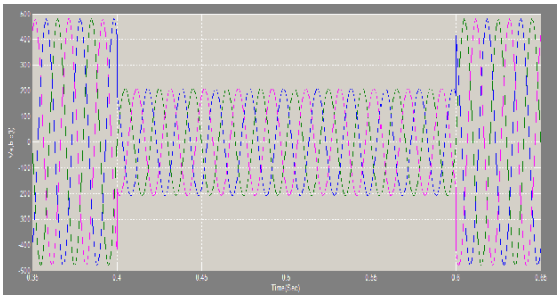

Fig. 10(a):

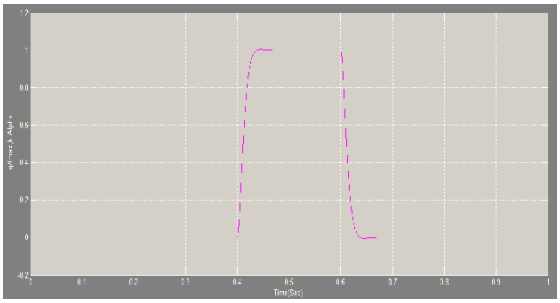

Fig. 10(b):

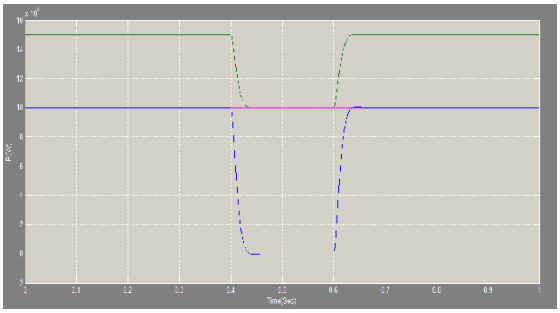

Fig.10(c):

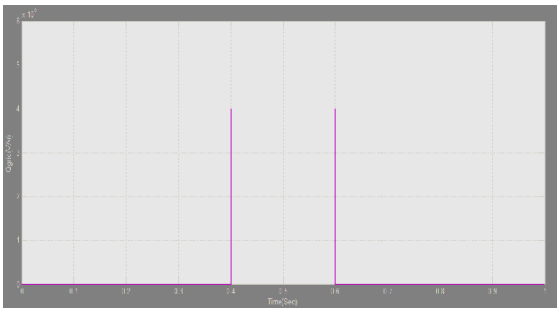

Fig. 10(d):

Fig. 10(a) PCC voltage, **(b)** Reactive powerreference factor (κ) the reactive current to rated GSC current ratio (*Iq/Im ax*) and(α), **(c)** Active power limitation (*Plim*) , active power reference (*P0 ref*), applied active power reference (*Pgrid ref*), and **(d)** GSC reactive power in symmetrical fault.

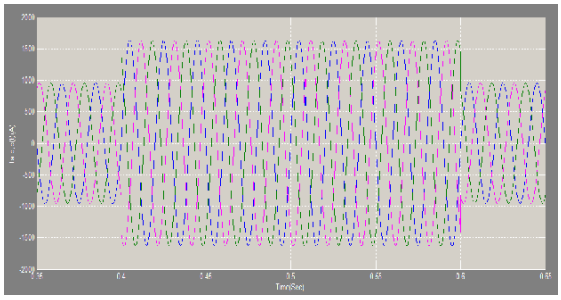

Fig. 11(a):

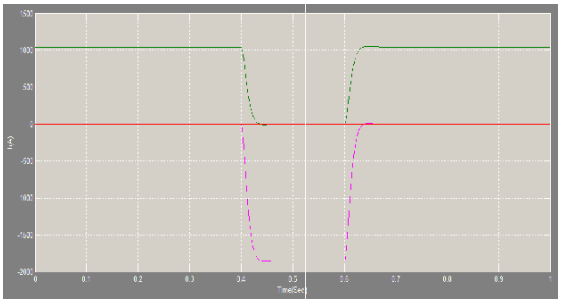

Fig. 11(b):

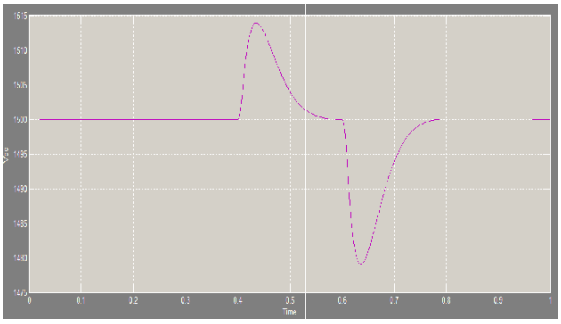

Fig. 11(c):

Fig. 11(a) Grid side c urrent, **(b)** The d-qcomponents of positivve- and negative-sequences of GSC current, and **(c)** DC-link voltage in symmetrical fa ult.

At the end, the symmetrical fault is simulated. According to Fig. 10(a), symmetrical voltage sag o ccurred 10 s that the voltage sag is more than 70%. As shown in Fig. 10(b), arising from the absence of a negative sequence component, α is equivalent with *Iqf+−/I*max, and they are one. Also, reactive power reference f actor κ is one. When this fault occurs, *Plim* approaches zero. Therefore, as shown in Fig. 10(c), *Pgrid ref* will be zero. Hence, the capacity of GSC is released and maximum reactive current will be injected to the grid. Fig. 11(a) shows the grid side current of GSC. All of the phase currents

were retained in the safe limit. A lso, Fig. 11(b) shows GSC current in the d-q reference frame. It is shown that the all capac ity of GSC is occupied by positive sequence of reactive current in fault condition. The prevention of dc-link overvoltage is the main advantage of the proposed method as shown i n Fig. 11(c).

In this system PR contro ller is used for fast switching response at asy mmetrical and symmetrical fault conditions . By using proposed controller, high accuracy is achieved.

CASE-1: ONE PHASE TO GROUND FAULT IS APPLIED (EXTEN SION)

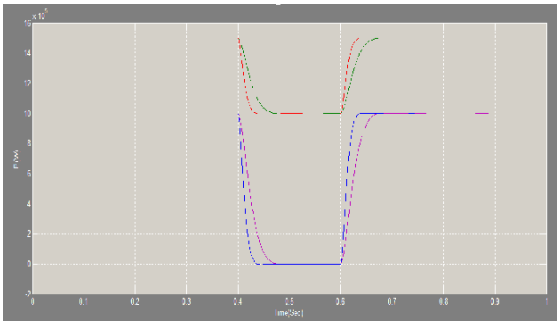

Fig. 12: Active power limitation (*Plim*), activepower reference (*P0ref*), applie d active power reference (*Pgrid ref* in one phase voltage sag (extension)

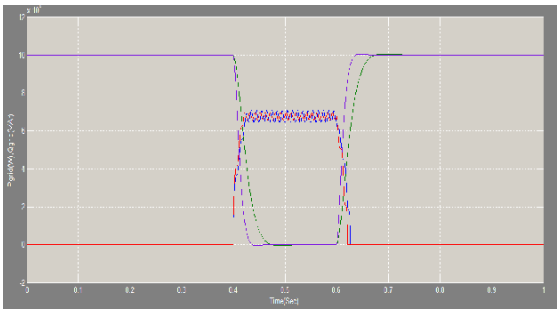

Fig:13: Grid active power and grid reactivepower in one-phase voltage sag (extension)

A one-phase to ground fault was applied to the PCC in 10 s. As shown in Fig. 12, the one-phase voltage sa g occurred in PCC. Fig. 12 shows the active power limitation (*Plim*), active po wer reference (*P0ref*), and applied active po wer reference (*Pgridref*) as MPPT controller input. In fact, the active power reference will be limited in safety bound when volta ge sag occurs in the grid, and allowable active power reference (*Pgridref*) is used as active power reference. As mentioned before, t o eliminate second-order component fluctuations of grid active power, *Pc*2 and *Ps*2 were set to zero; therefore, the second -order component fluctuations of grid active power is removed (see Fig. 13). But, the flu ctuations of reactive power of grid are retained . Hence, the reactive power oscillates with 100 Hz as shown in Fig. 13. It is important to not e that the average of reactive power in Fig. 13. Accordingly, reactive current injection is performed in agreement with the Danis h grid code.

CASE-2: TWO PHASE VOLTAGE SAG IS APPLIED (EXTENSIO N)

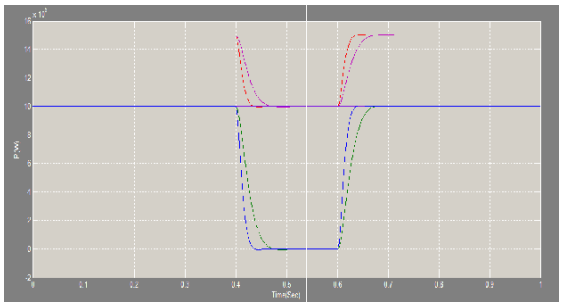

Fig. 14: Active power lim itation (*Plim*), activepower reference (*P0ref*), applied active power reference (*Pgrid ref*) in t wo phase voltage sag (extension)

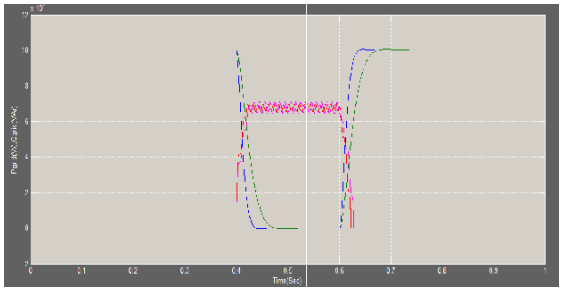

Fig. 15: Grid active pow er and grid reactivepower in two-phase voltag e sag (extension)

According to this scenario, unbalanced two phase voltage occurred in 10 sec. As earlier mentioned, the important issue is limiting the generated PMSG active power in grid side voltage sag. In this condition, the reference power does not track M PPT; see Fig. 14. In fact, the voltage drops c lose to 50%; Hence, the active current must be reduced to zero and

the GSC should inject reactive current equal to rated current of GSC. On the o ther hand, the second-order fluctuations of gri d active power will be removed as shown in Fig. 15. The*Qgrid* is similar to*Q*0 *ref* ; but it contains second-order fluctuations due t o the presence of negative sequence of curren t and voltage (see Fig. 15).

CASE-3: SYMMETRICAL FAULT IS APPLIED (EXTENSION)

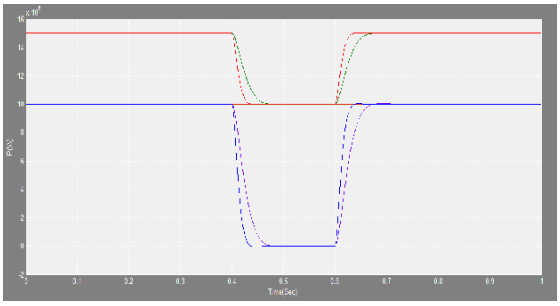

Fig. 16: Active power limitation (*Plim*), activepower reference (*P0ref*), applie d active power reference (*Pgrid ref*) in sym metrical fault(extension)

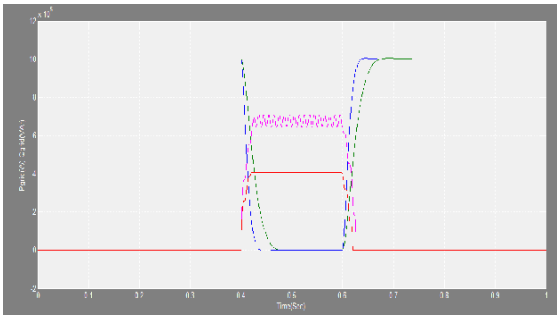

Fig. 17: Grid active power and grid reactivepower in symmetrical fault (extension)

At the end, the symmetrical fault is simulated. When this fault occurs, *Plim* approaches zero. Therefore, as shown in Fig. 16, *Pgrid ref* will be zero. Hence, the capacity of GSC is released and maximum reactive current will be injected to the grid.

For the future work, the proposed system can be improved in the control strat egy to enhance the system performance the interesting aspects could be the balanced power f low and their dynamic interactions in the system. In this system, The implementation of entire control system by using proportio nal resonant controller to reduce the computational time.

IV. CONCL USION

This project ha s presented a new method to enhance L VRT capability for PMSG-based wind turbin e during grid faults. The contributions of this work can be mentioned in two mai n concepts: dc-link overvoltage suppression by improving BTB converter controllers and design of active power limiter to maintain the peak current of the grid side inverter in a safe limit during different asymmetrical grid faults. The proposed BTB converter controllers and dynamic active power limiter possessed the following advantages: 1) there is no need to use external devices in grid fault conditions; 2) All GSC phase currents were kept within the safety limit in different grid fault conditions;

3) the negative sequenc e of current can be injected to grid, and the second-order active power fluctuation w as removed in asymmetrical grid faults; and 4) grid code requirement related to reactive current injection was performed. The current limiter has been derived by an a nalytical method by limiting the generated PMSG active power. Three different scenarios have been analytically presented and simulated to confirm the effectivene ss of the proposed control scheme.

REFERE NCES

[1] European Wind Enerrgy Association, EU Energy Policy to 2050— Achieving 80–95% emissions reductions. A report by the European Wind Energy Association, Mar. 2011.

[2] Energinet. Technical regulation 3.2.5 for wind power plants with a power output greater than 11 kW. Sep. 2010. [Online]. Available: http://www.energinet.dk

[3] M. Enamul Haque, Y. C. Saw, and M. M. Chowdhary, “Advanced control scheme for an IPM synchronous generator-based gearless variable speed wind turbine,” *IEEE Trans.Sustain. Energy*, vol. 5, no. 2, pp. 354–362,Apr. 2014.

[4] H.-S. Song and K. Nam, “Dual current control scheme for PW M converter under unbalanced input voltag e conditions,” *IEEE*

Trans. Ind. Appl., vol. 46, no. 5, pp. 953–959, Oct. 1999.
[5] J. F. Conroy and R.Watson, "Low-voltage ride-through of a full converter wind turbine with permanent magnet generator," *IETRenewable Power Gener.*, vol. 1, no. 3, pp.182–189, Sep. 2007.
[6] M. A. Asha Rani, C. Nagamani, G. Saravana Ilango, and A. Karthikeyan, "An effective reference generation scheme for DFIG with unbalanced grid voltage," *IEEETrans. Sustain. Energy*, vol. 5, no. 3, pp.1010–1018, Jul. 2014.
[7] M. Nasiri, J. Milimonfared, and S. M. Fathi, "A review of low-voltage ride-through enhancement methods for permanent magnet synchronous generator based wind turbines," *Renewable Sustain Energy Rev.*, vol. 47, pp.399–415, Jul. 2015.
[8] T. H. Nguyen and D. C. Lee, "Advanced fault ride-through technique for PMSG wind turbine systems using line-side converter as STATCOM," *IEEE Trans. Ind. Electron.*, vol. 60, no. 7, pp. 2842–2850, Jul. 2013.
[9] Z. Zhou, F. Scuiller, J. F. Charpentier, M. E. H. Benbouzid, and T. Tang, "Power smoothing control in a grid-connected marine current turbine system for compensating swell effect," *IEEE Trans. Sustain. Energy*, vol. 4, no. 3, pp. 816–826, Mar. 2013.
[10] S. Alaraifi, A. Moawwad, M. S. E. Moursi, and V. Khadkikar, "Voltage booster schemes for fault ride-through enhancement of variable speed wind turbines," *IEEE Trans.Sustain. Energy*, vol. 4, no. 4, pp. 1071–1081,May 2013.